Supporting Information

Enhanced Photoelectrochemical Performance of Quantum Dot-Sensitized TiO_2 Nanotube Arrays with Al_2O_3 overcoating by Atomic Layer Deposition

Min Zeng[a], Xiange Peng[a], Jianjun Liao[a], Guizhen Wang[b*], Yanfang Li[a], Jianbao Li[a], Yong Qin[c], Joshua Wilson[d], Aimin Song[d] and Shiwei Lin[a,b*]

[a] *Key Laboratory of Ministry of Education for Advanced Materials in Tropical Island Resources, College of Materials and Chemical Engineering, Hainan University, Haikou 570228, China*

[b] *Key Laboratory of Tropical Biological Resources of Ministry of Education, Hainan University, Haikou 570228, China*

[c] *State Key Laboratory of Coal Conversion, Institute of Coal Chemistry, Chinese Academy of Sciences, Taiyuan 030001, China*

[d] *School of Electrical and Electronic Engineering, University of Manchester, Sackville Street Building, Manchester M13 9PL, UK*

[a,d]*Corresponding Author: Prof. S. Lin. (linsw@hainu.edu.cn)

[b]* Corresponding Author: Prof. G. Wang. (wangguizhen0@hotmail.com)

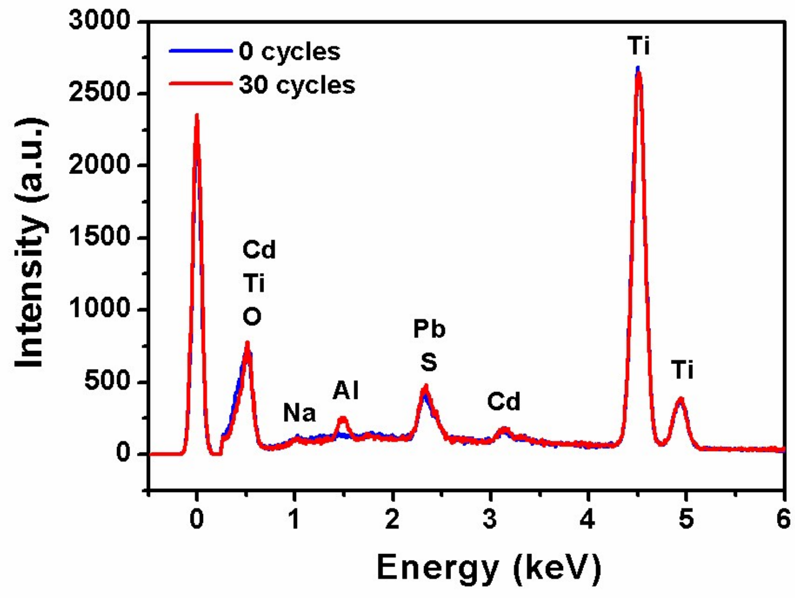

Fig. S1. EDS results of quantum dot-sensitized TiO_2 nanotube arrays without Al_2O_3 deposition (blue) and with 30 ALD cycles of Al_2O_3 overlayer (red). Na comes from the Na_2S used as the precursor.

Table S1. Atomic percentages of the elements derived from the EDS spectra in Fig. S1.

Photoanodes	Ti	O	Al	Na	Pb	Cd	S
0 cycles [%]	32.72	64.82	0.00	0.41	0.47	0.52	1.06
30 cycles [%]	35.07	62.19	0.67	0.00	0.45	0.44	1.17

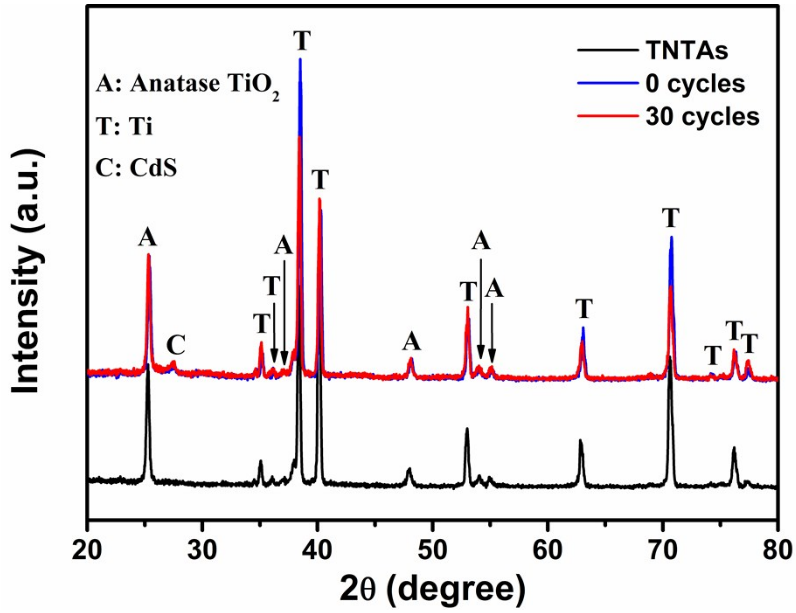

Fig. S2. XRD patterns of pure TiO_2 nanotube arrays (TNTAs, black), quantum dot-sensitized TiO_2 nanotube arrays without Al_2O_3 deposition (blue) and with 30 ALD cycles of Al_2O_3 overlayer (red).

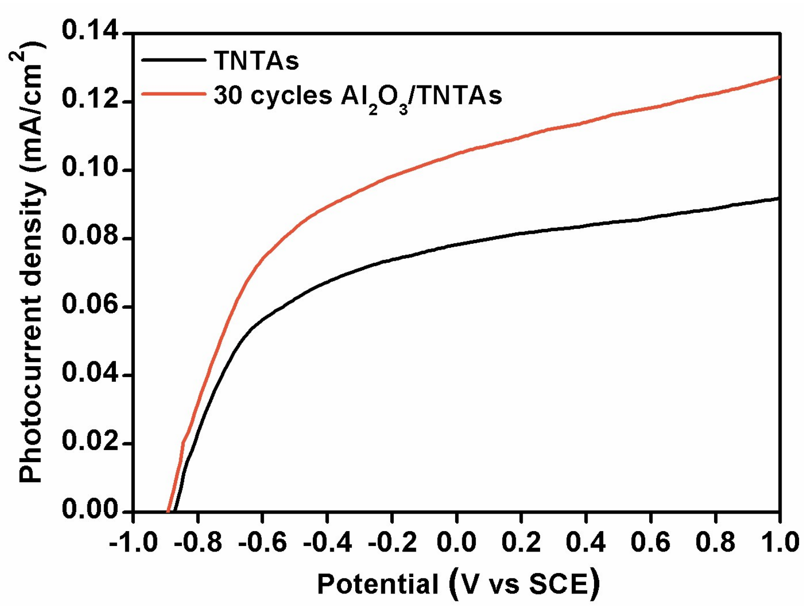

Fig. S3. Linear sweep voltammograms measured from pure TiO_2 nanotube arrays without Al_2O_3 deposition (TNTAs, black) and with 30 ALD cycles of Al_2O_3 (orange) under simulated solar illumination (100 mW cm^{-2}, AM 1.5 G) at a scan rate of 10 mV s^{-1}.

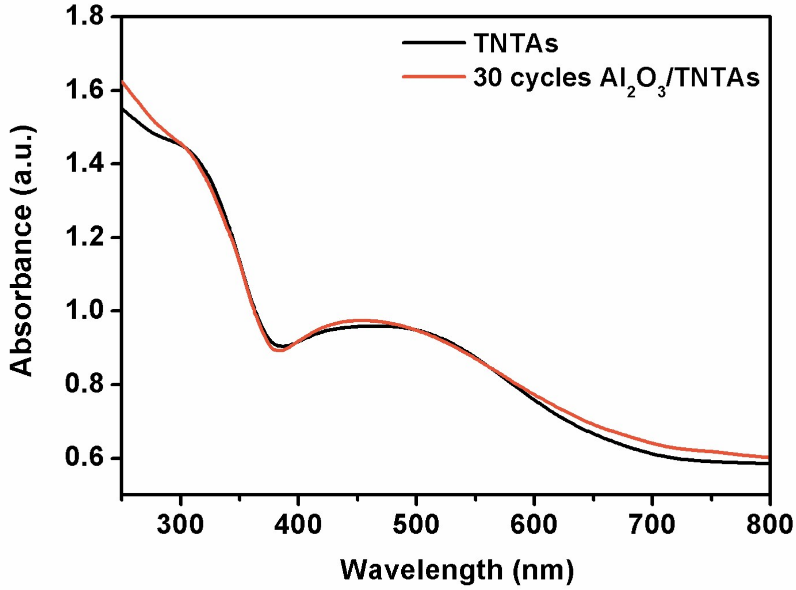

Fig. S4. UV-visible absorption spectra of the pure TiO_2 nanotube arrays without Al_2O_3 deposition (TNTAs, black) and with 30 ALD cycles of Al_2O_3 overlayer (orange).

Mott-Schottky analysis of photoanode:

The Mott-Schottky analysis was performed on quantum dot-sensitized TiO_2 nanotube arrays before and after Al_2O_3 deposition at a fixed frequency of 800 Hz with a perturbation amplitude of 10 mV and a scan rate of 30 mV s^{-1}. The electrolyte was 0.1 M Na_2SO_4 aqueous solution.

The Mott-Schottky equation correlates the inverse of the square capacitance with the donor density, N_D, and the flat band potential, V_{FB}, starting from Poisson's equation coupled with Boltzmann's distribution to describe the distribution of charges in the space charge region and Gauss' law relating the electric field at the interface [S1]. The Mott-Schottky equation is described by [S2]:

$$\frac{1}{C^2} = \left(\frac{2}{\mathrm{e}\varepsilon_0 \varepsilon_S N_D} \right) \left[(V - V_{FB}) - \frac{k_B T}{\mathrm{e}} \right]$$

where C is the space charge capacitance in the semiconductor, e is the elemental charge constant, ε_0 is the permittivity of free space, ε_s is the dielectric constant of the semiconductor, V is the applied potential, k_B is the Boltzmann constant, and T is the absolute temperature. The Mott-Schottky analysis of the space charge capacitance is performed in the linear region of the C^{-2} vs potential plot. A dielectric constant $\varepsilon = 48$ for TiO_2 is used to extract the flat band potential and the donor density of the photoanode without Al_2O_3 deposition (blue squares in Fig. S5) and the photoanode with 30 ALD cycles of Al_2O_3 overlayer (red triangles in Fig. S5) [S3].

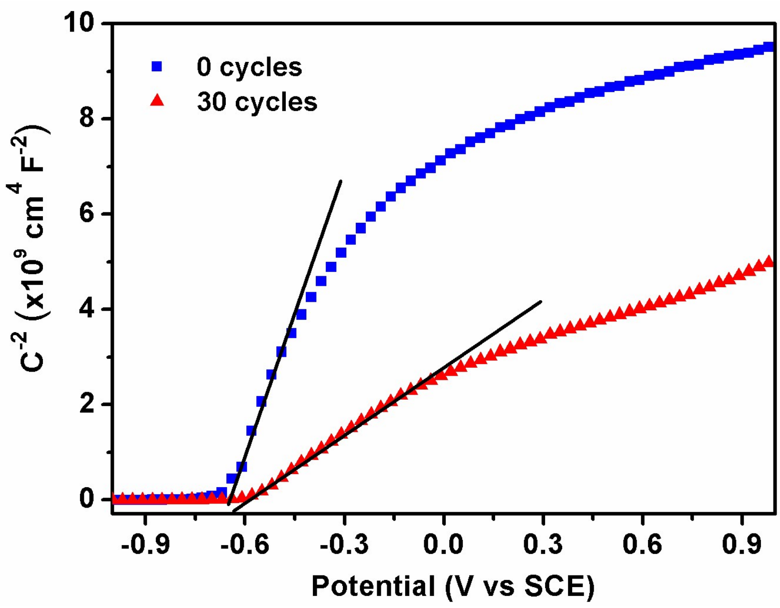

Fig. S5. Mott-Schottky analysis of quantum dot-sensitized TiO_2 nanotube arrays without Al_2O_3 deposition (blue squares) and with 30 ALD cycles of

Al_2O_3 overlayer (red triangles). The inverse of the square space charge capacitance is plotted vs the potential applied during the impedance measurement.

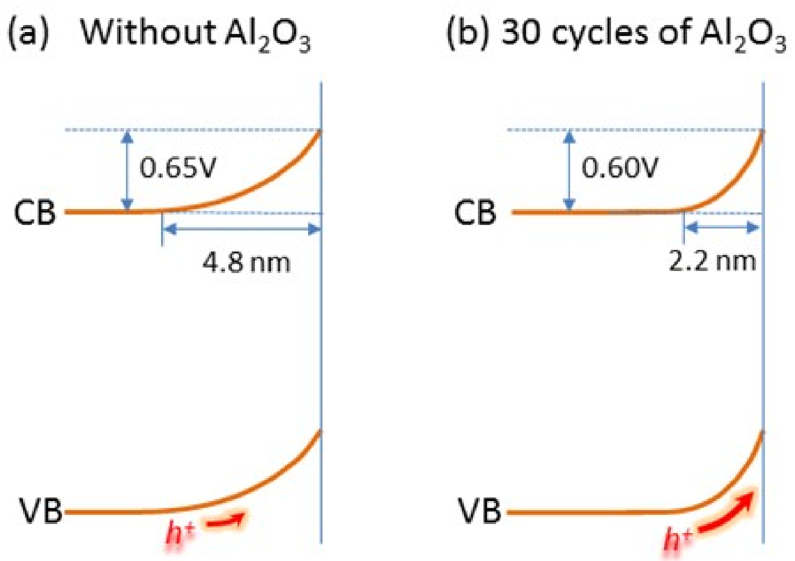

Fig. S6. Schematic band diagrams near surface based on the calculated electronic parameters for the photoelectrodes (a) without Al_2O_3 deposition and (b) with 30 ALD cycles of Al_2O_3 overlayer. The size of the arrow presents the strength of the effect from built-in electric field.

Table S2. EIS fitting results.

Photoanode	R_s/Ω	R_{ct}/Ω	CPE/F
0 cycles	9.0	207.8	1.9×10^{-3}
30 cycles	8.8	145.0	2.4×10^{-3}

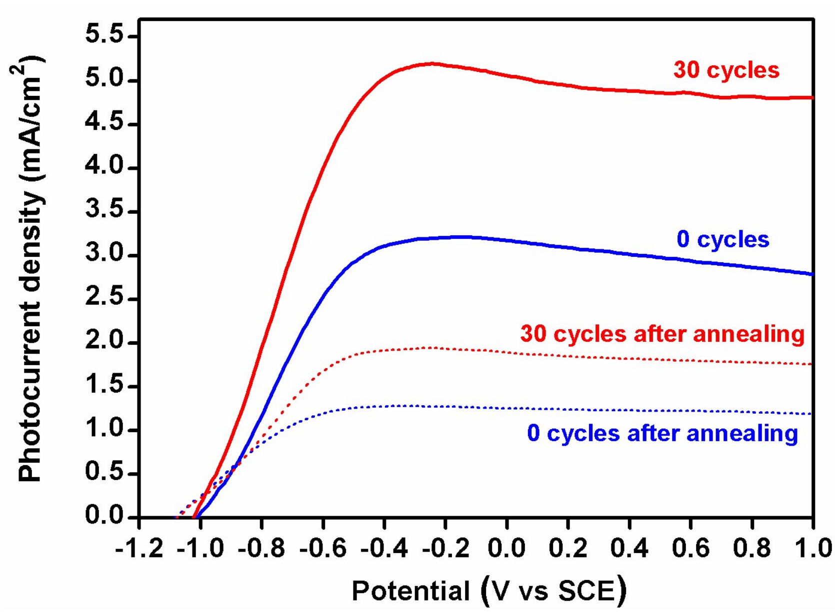

Fig. S7. Photocurrent density-potential curves of quantum dot-sensitized TiO_2 nanotube arrays with 0 cycles (blue) and 30 cycles (red) of Al_2O_3 overlayer before (solid lines) and after (dot lines) annealing at 400 °C.

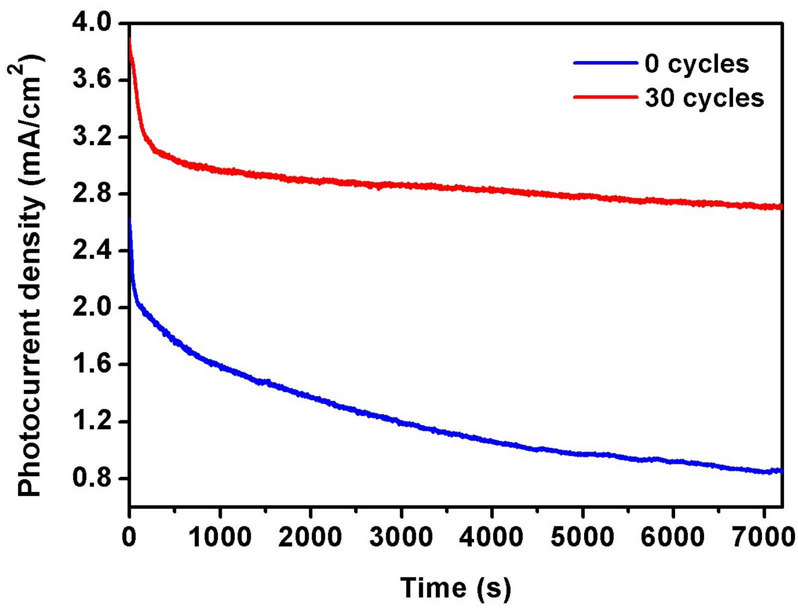

Fig. S8. Time-dependence photocurrent density of the quantum dot-sensitized TiO_2 nanotube array photoelectrodes without Al_2O_3 deposition (blue) and with 30 ALD cycles of Al_2O_3 overlayer (red).

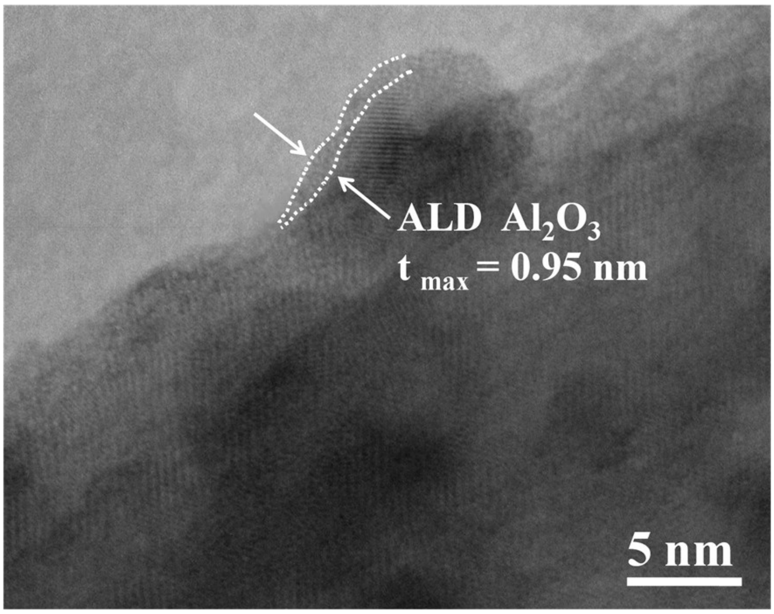

Fig. S9. High-resolution TEM image of quantum dot-sensitized TiO_2 nanotube arrays with 30 ALD cycles of Al_2O_3 overlayer after PEC test.

References

[S1] F. Le Formal, N. Tétreault, M. Cornuz, T. Moehl, M. Grätzel, K. Sivula, *Chem. Sci*. 2 (2011) 737-743.

[S2] A. Wolcott, W. A. Smith, T. R. Kuykendall, Y. Zhao, J. Z. Zhang, Adv. Funct. Mater. 19 (2009) 1849-1856.

[S3] M. Ye, J. Gong, Y. Lai, C. Lin, Z. Lin, *J. Am. Chem. Soc*. 134 (2012) 15720-15723.